Designing an apparatus for measuring bidirectional reflection/transmission

Peter Apian-Bennewitz

Fraunhofer Institute for Solar Energy Systems
79100 Freiburg, FRG

ABSTRACT

An apparatus for measuring angle-dependent transmission and reflection of large (40x40cm) samples is presented, and details of the optical, mechanical and computer aspects given. The apparatus consists of two fixed light sources, an adjustable sample holder and a movable solar cell as the detector. All angle positions are computer-controlled, using a workstation to achieve automatic measurements. Data-processing steps for large and small samples are presented.

1. INTRODUCTION

Data on the scattering of light in window materials is needed for a number of applications: e.g. daylighting[456], design of collector front covers[3] or theoretical modelling of light transport inside materials. The scattering is described as a bidirectional reflection/ transmission function (BRTF), which specifies how much of the incident light is scattered in a given outgoing direction. Generally the BRTF can be written as: BRTF($\mathbf{x}_{in}$, $\mathbf{p}_{in}$, λ_{in}, $\mathbf{x}_{out}$, $\mathbf{p}_{out}$, λ_{out}, $\mathbf{xy}$) with $\mathbf{x}$ the directions of the incident and outgoing light, $\mathbf{p}$ the polarization vector, λ the wavelengths, $\mathbf{xy}$ the position on sample. Depending on material symmetry and homogeneity, the number of BRTF parameters can be reduced. A typical BRTF for wavelength-independent (grey), homogeneous samples would be written as BRTF(θ_{in}, ϕ_{in}, θ_{out}, ϕ_{out}) using the coordinate system shown in fig. 11.
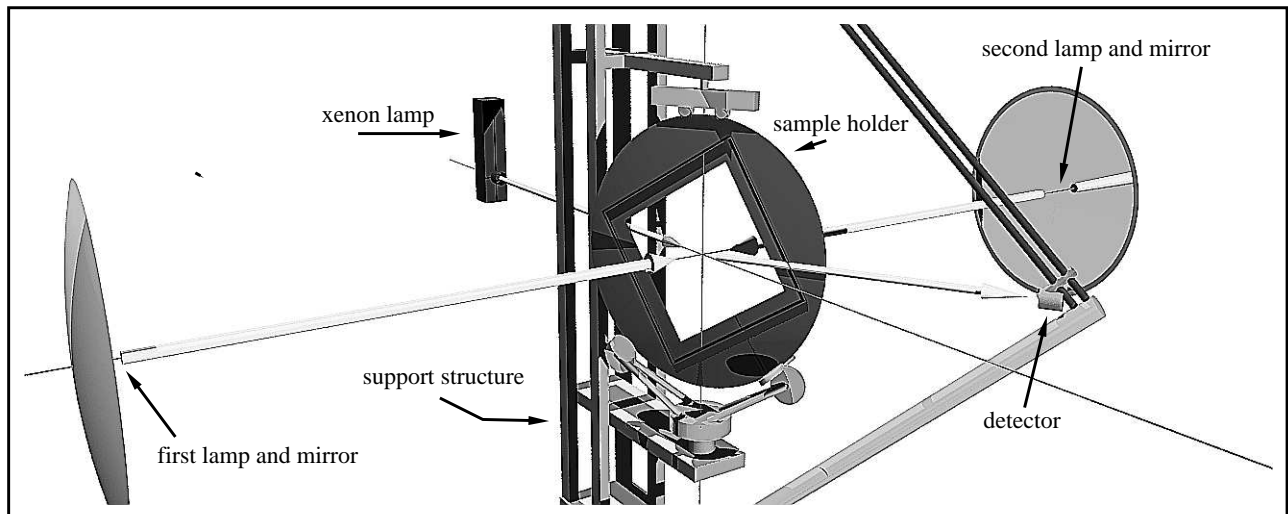

Fig. 1. Layout of sample holder, detector and light sources

2. GENERAL LAYOUT

An experimental set-up[1] for measuring BRTF's consists of a light source, sample holder and detector. A number of different geometric configurations is possible, each offering every combination of incident and outgoing light directions: Classical set-ups consist of one movable lamp and one detector, the more common one uses one fixed lamp, a movable sample holder and one movable detector, an exotic design could trade mechanical complexity for the number of lamps or detectors, arriving at a detector grid or array or a ring of lamps. The following design features two fixed lamps with a reduced scanning area for the detector as sketched in fig. 2.

The main parameter determining the overall dimensions of the apparatus is the sample size, 40x40cm^2 in our case. To illuminate these large samples with parallel, homogeneous and intense light, a parabolic mirror was used. The size of the mirror favoured a fixed mounting, so the sample holder has to turn the sample to change the incident light direction relative to the sample. Since the incident light direction is specified by two angles, the sample holder has to have two degrees of freedom or two axes, which are

described in detail later. The distance to the detector depends on the type of detector used and was set to 1m, allowing the whole apparatus to fit into a room of 2.9m height. Measurement time was estimated to be on the order of hours, so the apparatus was designed for continuous, automated measurement with motor control for all axes.

To facilitate software development and remote operation, a UNIX workstation is used as the controlling host computer. For the mechanical drives cog belts were preferred to worm-gears. They require no precise alignment or lubrication, their friction is load independent and they provide the reduction needed. All axes are driven by 5-phase stepping motors with an angular resolution at the motor axis of 0.36 degree/step. The power is supplied to the motors by a 20A three-phase transformer/rectifier to allow all four motors to be started at once. A closed-circuit loop interrupts the power supply if an axis is going to hit the mechanical limit, in case the checks built into the lower software layers fail.

As with all stepping motor drives, the controller has to find the absolute position at the start or after a power break. Therefore light barriers are mounted in the middle of each axis and the zero positions are defined relative to them. No absolute or relative angle encoders have been used, trusting that a well-powered drive will not lose steps unless something is blocking its way. The latter is recognised when a motor should have crossed a light barrier on its way but fails to do so.
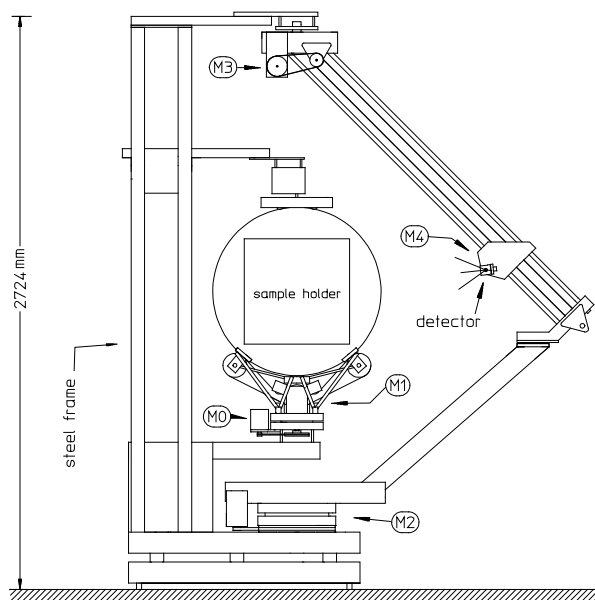

Fig. 2. Schematic side view of the sample holder and detector. M0 to M4 are the stepping motors

3. DETAILS OF HARDWARE DESIGN

3.1. Lamps

The ideal lamp should produce parallel, homogeneous illumination across the sample area with a solar-like spectrum. For large samples (40x40cm^2) a halogen lamp and a front surface coated, parabolic mirror (lighthouse mirror) was used. Although halogen lamps do not match the solar spectrum well, they are smaller than xenon lamps, have a wider angular output and do not require mechanical shielding. The lamp bulb was mounted in the mirror focus using a steel wire system to minimize shading. To avoid shading completely, an off-axis parabolic mirror could be used. However we estimated that the induced error could be later compensated for by data processing. A battery is used as the power source, providing purely direct current, while an electronic switch (FET) allows computer control.

For transmission measurements on small samples (4x4cm^2) a 1kW Xe lamp produces an 18mm diameter beam, using a 0.8mm pinhole and a photographic lens (f=125mm) to provide a parallel beam with a gaussian cross-section. The light intensity is stabilized by a photodetector and feedback circuits to the power source. A mechanical shutter allows control by the host computer.

3.2. Sample holder

The sample has to be turned around two orthogonal axes, one perpendicular to the incident beam. In this set-up the first axis is mounted vertically for mechanical reasons. The second axis could either be parallel to the sample surface or perpendicular to it: the latter avoids shadows cast by the mechanical hinge on the sample. The sample holder consists of an 800mm diameter aluminium disc, 5mm thick, with a 500x500mm^2 hole at the center. T-shape aluminium mouldings are mounted around the square hole, giving mechanical stiffness and a mounting frame for the inner sample holders. Various sample sizes and shapes have their own "inner" custom mounting.

The aluminium disc rests on two rollers which are connected to the stepping motor by a cog belt. Slip during acceleration between the belt and the disc is not a problem, however experience suggests that a design with some "teeth" synchronisation between the disc and the drive would prevent drift for long movements without rezeroing. The precision for this axis is approximately 19 steps/degree.

The disc and its drive are mounted on a turntable driven by a second motor over a 1:5 cog belt reduction with 14.3 steps/degree. Experience shows that for higher precision in the incident angle, a 1:5 planetary gear should be added, as the original design laid more emphasis on speed than turned out to be necessary for this axis. Since power to the disc motor is supplied by a cable rather than problematic collector rings, rotating the turntable more than 370º should be avoided. To ensure this, even if the software fails, the power is cut by the short-circuit power-off loop if the allowed angle range is exceeded.
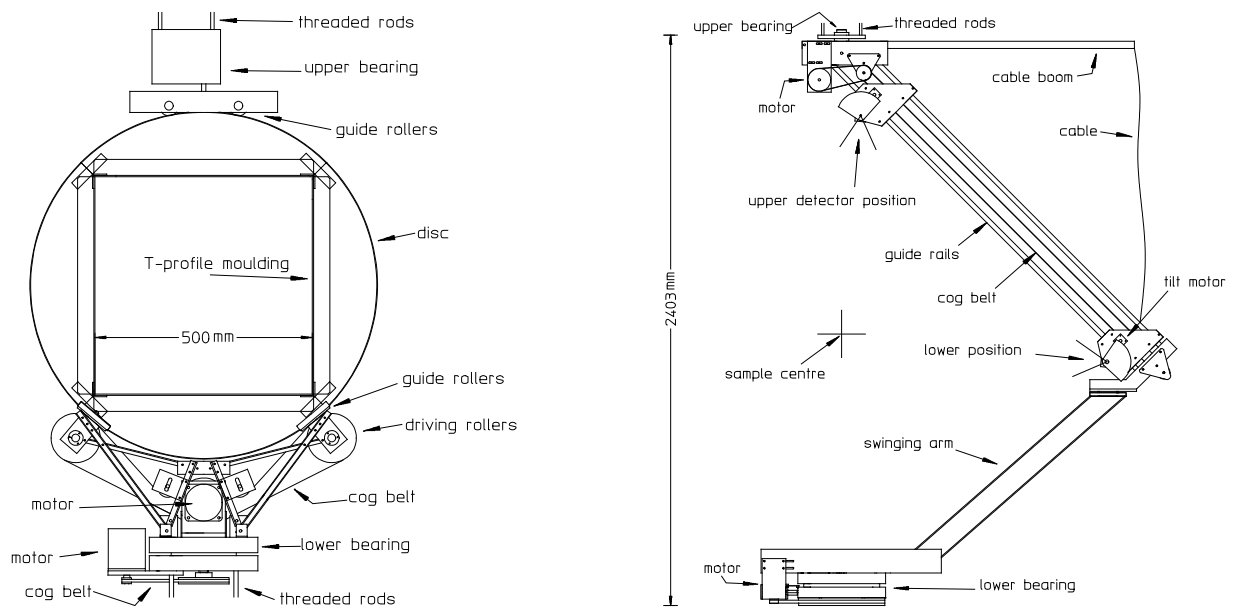

Fig. 3. Sample holder and detector hinge

3.3. Detector connection

As with the sample holder, the detector is moved around two axes, one vertical, one horizontal. At first sight it would seem that the detector has to scan a 4π solid angle around the sample to measure reflection and transmission. This is halved due to the rotational symmetry around the incident light direction, because there are two equivalent sample positions. Further reduction would be possible with a third degree of freedom added to the sample holder, but would also add considerable mechanical complexity. A second lamp offers two more, equivalent sample holder positions, reducing the detector scan angle to π steradian (a quarter sphere).

The detector is not moved below the sample centre, allowing a rigid support structure up to this level. Also the detector is not moved along a circle but a straight line, taking advantage of linear bearings as reliable, cost-effective, off-the-shelf products. The varying distance to the sample centre is accounted for by software (see chapter 5 for details). A carriage is used for the vertical movement of the detector to avoid problems associated with rotation of long, freely suspended arms (inertia, angle resolution, resonance frequencies), especially during start/stop acceleration.

Along the 2m long rails the detector is moved by a cog belt, mounted and tensioned at the detector carriage and connected to the motor with a slight reduction, giving a resolution between 108 (for 45º) and 212 (for 0º) steps/degree, or better than 0.5'/step. Keeping the detector mounting "thin" minimizes the shadow cast on the sample while measuring reflection near the incident direction. A fifth two-phase stepping motor tilts the detector to point at the sample centre (5 steps/degree). The whole detector system is rotated around a vertical axis by a turntable with 1:42 reduction and 118 steps/degree, appr. 0.5'/step resolution. The maximum speed is 180 degrees in 5 seconds.

3.4. Detector

The apparatus uses a $2x2cm^2$ solar cell as a detector; its short-circuit current is measured with a Keithley 485 Picoammeter. Since most measured results are used for daylighting and photometric simulations, a green $V(\lambda)$ filter adapts the spectral sensitivity to the photopic response. The acceptance angle of the detector is designed for full view of a $40x40cm^2$ sample (maximum 39º). Clearly, with a fully lit $40x40cm^2$ sample the outgoing light is not parallel and the measured data has to be corrected (see 5.2). While it would be possible to restrict the acceptance angle of the detector to a few degrees by lenses, a diaphragm at the sample is preferred to avoid aiming problems with the detector. The problem of large lit samples could also be addressed by an angle-resolving detector, for example a CCD camera. Tests showed problems with the dynamic range, automatic gain control, blooming and resolving power of a specially designed CCD camera which would require further investigation. The correction of measured data is easier if the smaller beam of the xenon lamp is used and the thickness of the sample guarantees a small area of outgoing light. In that case, the minimum detector distance (0.7m) is large enough compared to the light emitting area ($\varnothing$ 0.018m) to use an inverse-square-law correction.

Currently the speed of the Keithley 485 (2-4 measurements/sec) limits the angular resolution (see 4.2), an upgrade to a faster analog/digital converter is planned. The ammeter is run in fixed range mode to avoid unforeseeable time delays while the instrument switches ranges. If an overflow or underflow occurs during measurements, that area is rescanned with an adjusted scale.

3.5. Alignment

All turntables and bearings are adjustably mounted on to a steel "backbone", allowing tolerance in the welded steel structure. Alignment is simple using a lead plumb, water level and laser, since all the main axes are either horizontal or vertical. The lowest detector hinge bearing is levelled so that the detector support structure rotates in a horizontal plane; the vertical axes are then aligned by starting from the lowest bearing upwards. The beam of a wall-mounted small HeNe laser runs horizontally through the sample centre and defines a zero axis for both the sample holder and the detector. Rigidly mounted, it also serves as a periodical alignment check. The reductions are easily calculated and checked with a 180º or 360º rotation. As with nearly all reductions, the cog belt drives together with friction in the bearings cause a misalignment when the same position is approached from two directions (backlash). This was checked using an axis mounted mirror and a laser beam. For the detector axis this was found to be smaller than a step, due to the tensioned cog belts and a large roller bearing with lower friction. The worst case is the sample holder vertical axis with 2-3 step backlash. The sample disc drive suffers from drift (compensated by rezeroing) but shows no backlash, neither does the carriage drive (gravity and belt tensioning).

4. DETAILS OF THE HARDWARE AND SOFTWARE

4.1. Hardware interface

Selecting a UNIX workstation as the host computer suggested the use of the VME bus system as an interface to additional hardware. This bus features a wide variety of boards and manufacturers, speed (20MByte/sec) and multiprocessor ability. Two additional microprocessors control the five stepping motors, using single-board microprocessor systems with CPU, RAM and timers (68000 derivative, 128KByte RAM, EPROM resident monitor program, 3 Zilog timers). Optocouplers between these boards and the stepping motor power control hardware ensure voltage protection and avoid ground loops in the control lines (5-10m cable length). Communication between the microprocessor boards and the host computer is done via the VME bus, or via serial (RS232) interfaces as an emergency link. During software development and while monitoring a measurement, more than one program can communicate with the motor-control boards (e.g. position monitoring); these overlapping accesses are handled by the hardware without further user involvement. Feedback from the set-up (zero positions) is fed through the motor-control boards to the UNIX side.

The software running on the motor-control boards was developed by the author and controls up to three motors per board with the necessary acceleration ramps, zero checking and error trapping. The code resides in RAM and is downloaded into the boards from the host computer after power-on. The standard software moves the motors simultaneously, for example to reach a given detector or sample position, while a newly developed version allows the detector or sample to be moved on a predefined path, for example to use the sample holder as a "sun-machine", simulating the sun's course for a given day and location.

4.2. User program interface

An additional software layer is required between the programs running on the motor-controller boards, written in assembler language and accessed via the VME bus, and the user program governing the measurement procedure, written in C. This layer consists of a number of subroutines grouped together in a library handling error-checking, degree/motor-step conversion and position feedback. Similar libraries provide control routines for the Keithley picoammeter and the transformations between the coordinate system of the detector movement and the sample.

Most measurement procedures take data "on-the-fly", gathering values as rapidly as possible while the detector rotates around its vertical axis (called a "sweep"). The resolution is given by the detector speed and the analog/digital conversion time of the ammeter. It varies between 0.1 (taking data on the beam profile) and 2 degrees (e.g. for aerogel samples). After one "sweep", the detector's vertical position is raised by moving the carriage up (0.1 to 5 degrees) and the detector is swept back.

This algorithm is well suited for forward scattering materials showing no pronounced peaks in their output distribution (e.g. aerogels, frosted glass). An angular resolution of 2-5 degrees is sufficient and a complete scan takes between 5 and 15 minutes. By contrast, samples like Transparent Insulation Material (TIM) honeycomb structures[2] or shading devices (fixed blinds like "Okasolar") show strong specular transmission or reflections and are not well served by fixed resolution data gathering. Either the angular resolution is too coarse and peaks are missed, or the time needed for full sweeps with fine resolution is too long; so an adaptive refinement method was added: During a coarse pre-scanning (1.5 degrees), "interesting" angular areas are identified, either based on high values (e.g. above 75% of maximum) or slope (rapidly changing intensities). A second scan measures these areas at an increased angular resolution. This method was especially used for honeycomb materials as illustrated in fig. 8.

5. DATA PROCESSING

5.1. Small samples

Background subtraction, detector distance correction and cosine corrections for incoming and outgoing areas are done by a second program, writing data files for use in fitting programs or plotting packages. Currently the data is checked using a standard two-dimensional plotting package (gnuplot or unigraph) or a workstation with special display hardware to analyse the BRTF in three dimensions: Intensities are shown as a "mountain" defined over a projection of the hemisphere onto a plane as shown in fig. 4. The display hardware allows interactive rotation and analysis. Since only the solid angle of a quarter sphere is scanned, the data "mountain" is only half of what might be expected (cf. section 3.3): the second half is symmetric for rotationally symmetric materials. Contour bands are blended into the image at 10, 20,30.. percent of maximum intensity. Curves of constant θ_{out} are circles, radial lines are the loci of constant ϕ_{out}. The grid on the base plane is in steps of 10° for θ_{out} and ϕ_{out} . Measured points are displayed as small spheres. Cross sections of typical "mountain" datasets are plotted in fig. 7.

/nfs/koll3/users/koll/tmess/data/joule2/prod3/dc/ho4121-0.dc min= -8.02136e-05 max= 0.383452

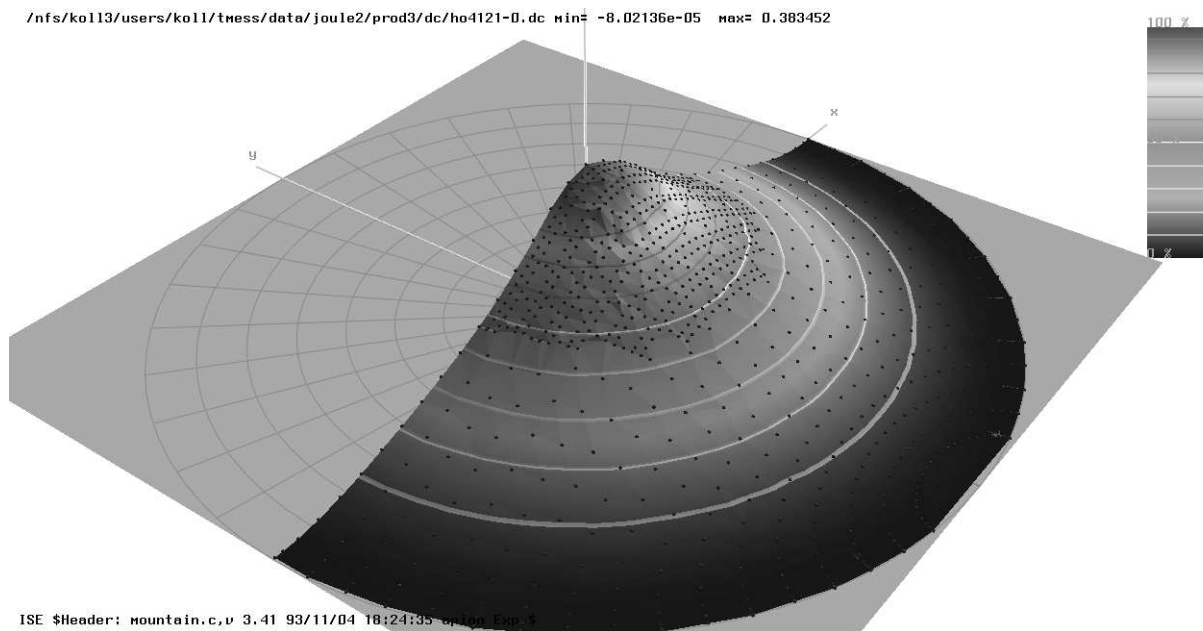ISE $Header: mountain.c,v 3.41 93/11/04 18:24:35 opion Exp $

Fig. 4. Forward scattering data shown as a 3d "mountain" on a workstation display

Scanning the angular distribution with one detector "sweep" determines that data sampling is not done at a constant theta-phi grid in the sample coordinate system. While this is irrelevant for fitting programs, some further data processing may be hampered, and necessitates an interpolation. Delauney triangulation and linear interpolation turned out to be most stable and reliable, while other fit methods may produce artificial "holes". The triangulized net can be displayed on the workstation: fig. 5 shows the measured points as small spheres, "sweeps" appear as lines on the left hand side; the higher values on the right hand side are measured with a finer resolution.
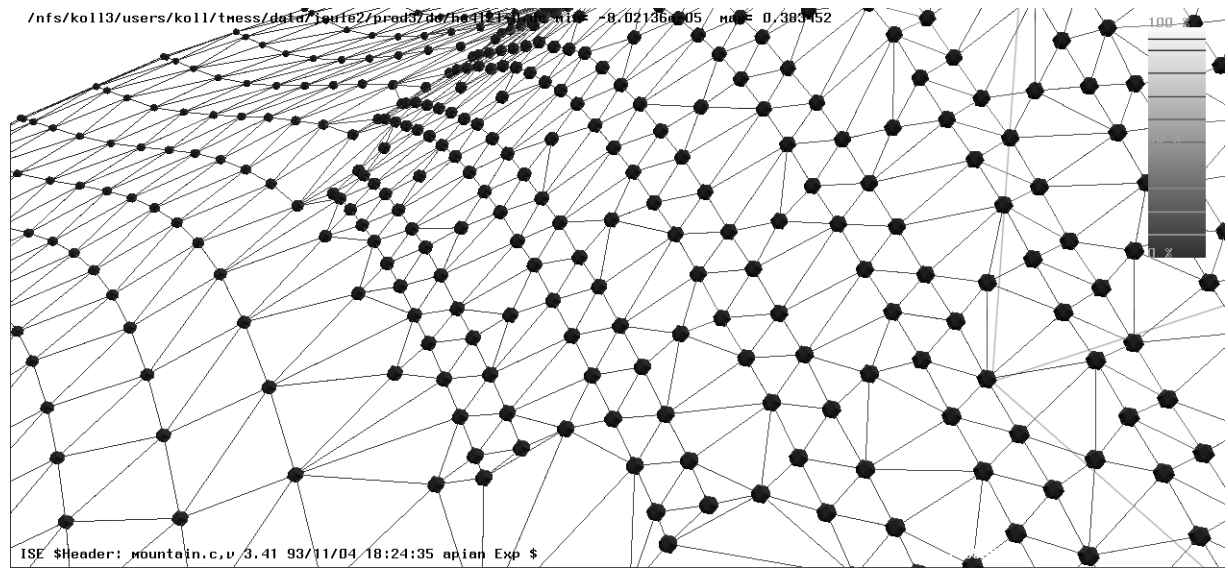
Fig. 5. Triangulation of measured points for display and interpolation

As of this writing, no integration of the spatial transmission data has been done, as modelling of the spatial distribution was of primary concern. Future work will link this data to measurements made with integrating spheres.

5.2. Large samples

Generally, for arbitrary materials, it is not possible to calculate the BRTF from the illuminance distribution measured with a detector at finite distance which, in this case, is only about twice the sample dimensions. Adding some assumptions about the emitting surface however makes such a reduction of the data possible.

In a first approach, an explicit model for the light distribution was assumed, e.g. a cone-shaped output follows from theoretical analysis for TIM honeycombs. This model was parameterized (e.g. cone height, width and offset), the resulting light distribution on the detector surface calculated and the model fitted to the measured data. While this presents no difficulties in the mathematical process, it is only possible if at least a crude model is available.

Further investigation[7] showed that data reduction is also possible assuming only homogeneity and optical thinness of the material. The detector signal is again treated as a weighted sum of small patches of the sample surface, but the angular distribution at each patch is written as a discrete vector. This, as yet unknown, vector is matrix multiplied to yield the measured light distribution vector. The matrix consists of the known sample and detector geometry and each measurement defines one line in a vector equation. This leads to a system of linear equations. Standard matrix inversion methods fail because each measurement incorporates some unavoidable errors and fluctuations, which blow the matrix solutions to wild singularities. Regularization[8] was used successfully to implement a more robust inversion method leading to smooth solutions for the scattering vector. This was done for two-dimensional scattering in a plane and the extension to full 3d scattering does not appear to be a problem in principle. Figure 6 shows a comparison between the measured data (solid line) and the reduced data (dashed line); the broad peak in the middle is due to a pronounced delta peak in the BRTF, smeared by the geometry of the finite detector. The regularization recalculates the original BRTF peak.
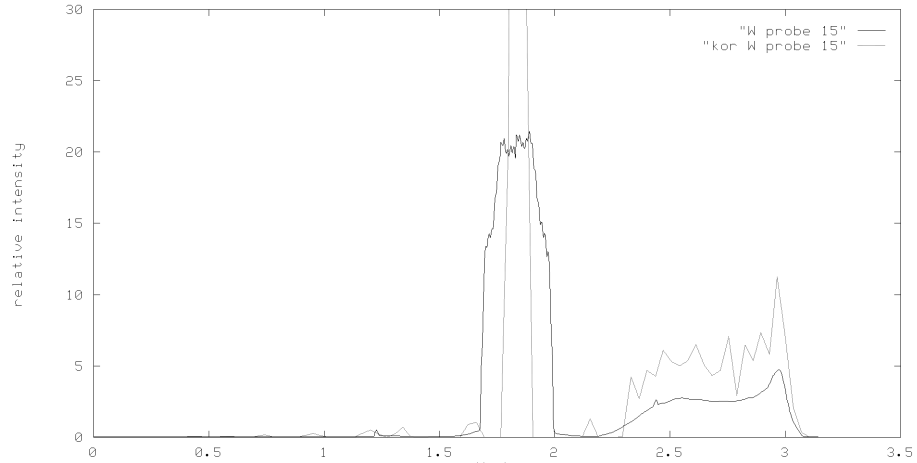
Fig. 6. Measured scattering data for one incident angle and the corrected BRTF. X axis scale is in [rad]

6. EXAMPLE RESULTS

6.1. Forward-scattering materials

Figure 6 shows a comparison between four different materials for normally incident light: a thermotropic material[9] ("Suntek") heated above the switching point to 32° C, two layers of drawing paper, a polymer material between glass plates and a single layer of drawing paper. The data is corrected for the sample-detector distance and divided by $\cos(\theta_{out})$, so an ideal lambertian emitter would be drawn as a horizontal line. Also plotted are the fitting functions, in this case a sum of four $\cos^n(\theta_{out})$ terms.
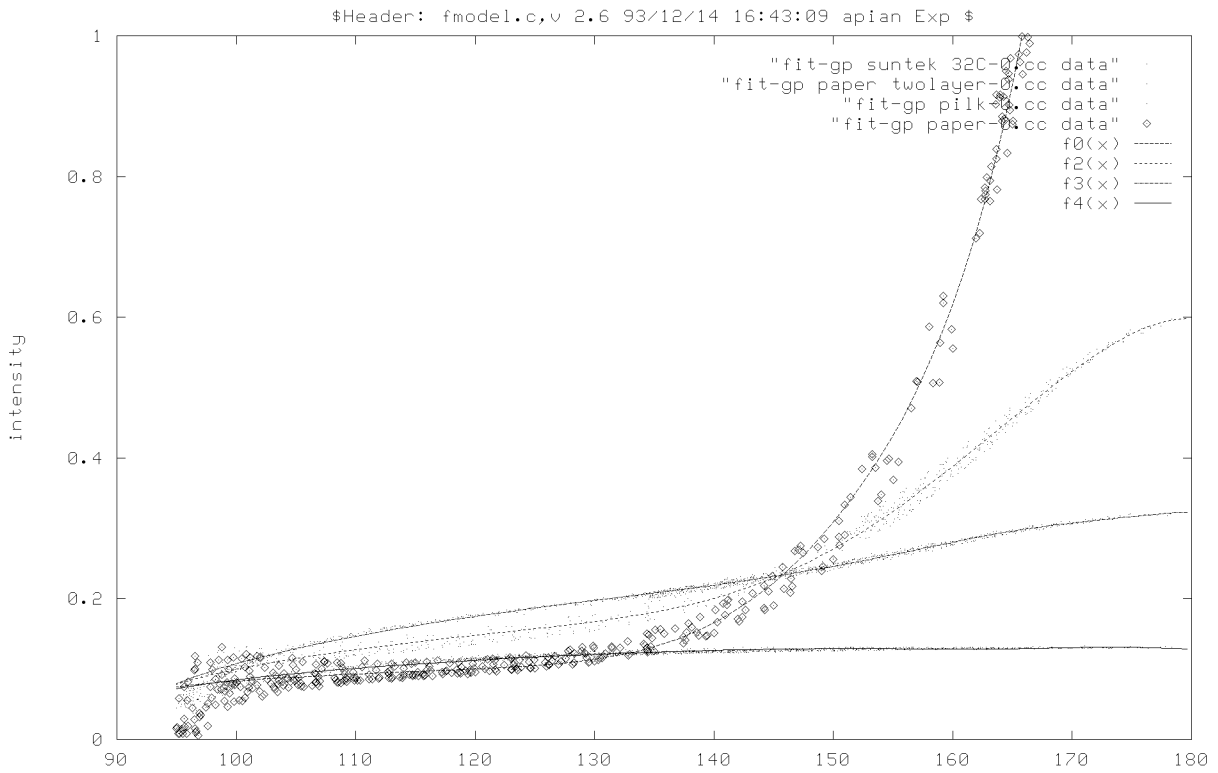
Fig. 7. Forward scattering data for different materials; relative intensities versus θ_{out} [degrees]

6.2. TIM honeycomb materials

As an example of TIM honeycomb materials, data from a sample made of glass cylinders with a diameter of 6mm and a wall thickness of 0.1mm is shown in fig. 8 and 9. As for all honeycomb structures, the incident light is scattered in a cone shaped ring with an opening angle equal to the incident angle. The white bands are iso-intensity lines at 10, 20, 30,... percent maximum intensity. The peak on the right side of fig. 8 represents light leaving the material in the forward direction.
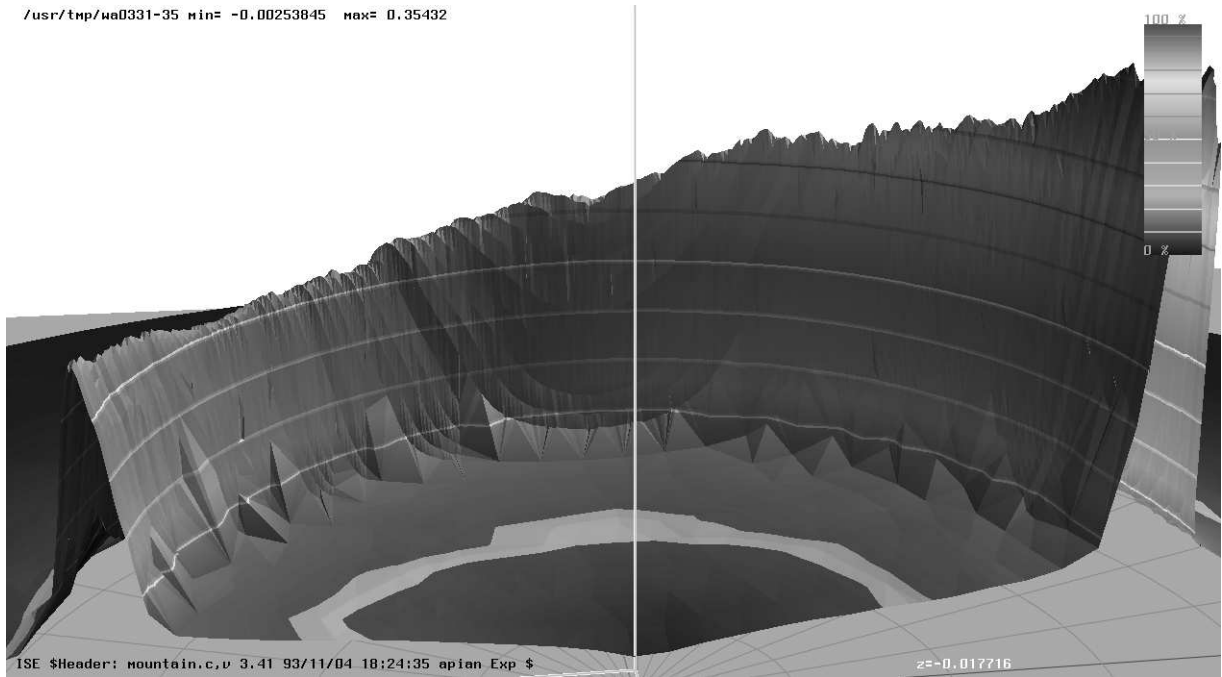
Fig. 8. Light "ring" of a TIM honeycomb structure with glass capillaries; incident angle is 35º
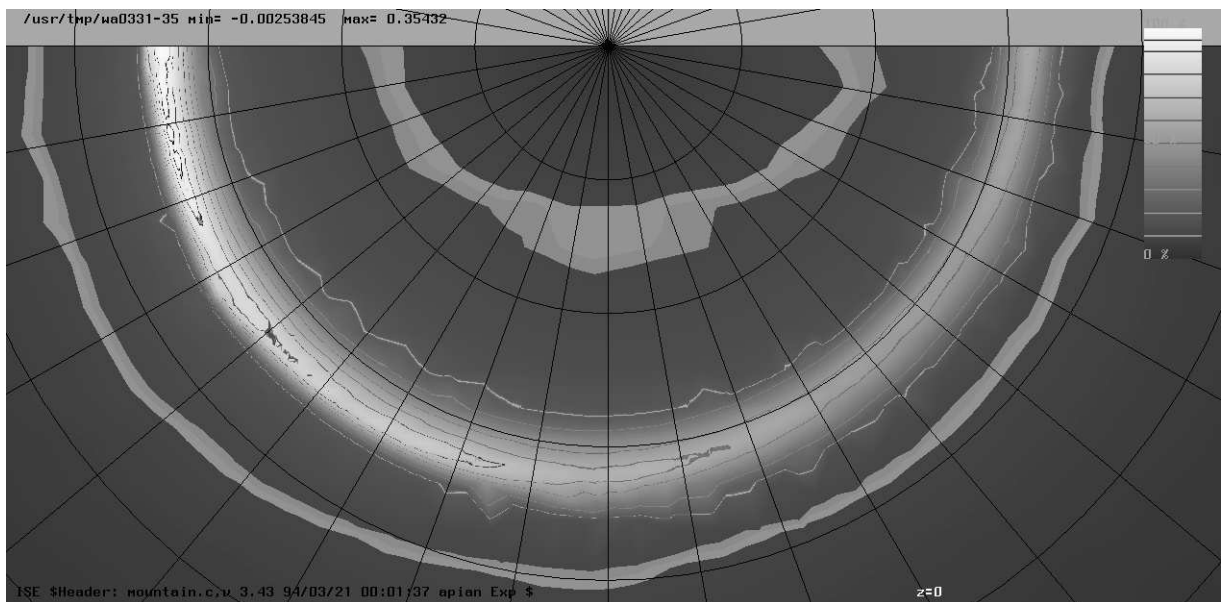
Fig. 9. Polar plot of same sample as fig. 8, black lines are a 10º step θ/φ grid, the inner and outer rings are the 10% lines

6.3. Reflection

To check theoretical calculations for integrating sphere coatings, measurements were made on Teflon materials, a test coating mixture of Teflon and coal to vary the overall reflection. The specular peak (incident angle = outgoing angle) is visible on the left side of fig. 10 for an incident angle θ_{in}=60°.
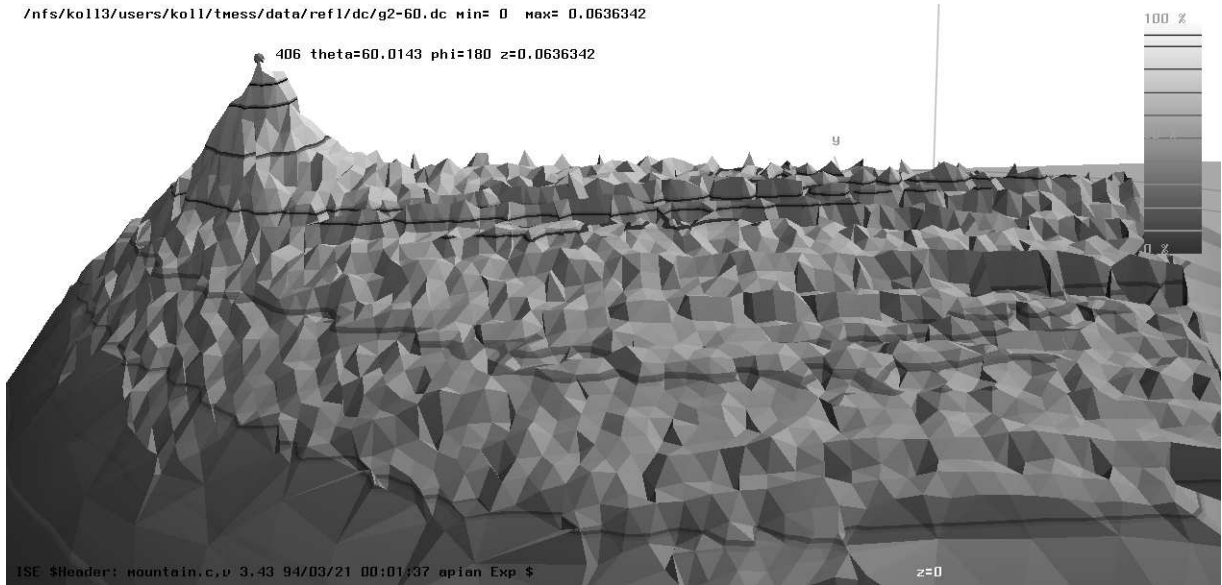

Fig. 10. Reflection showing the specular peak at θ_{out}=60°; the material is a teflon/coal mixture

6.4. Beam profile of Xenon Lamp

The beam profile of the small beam xenon lamp was measured to develop a method for calculating the total incident radiation: Figure 11 shows the results of the scan, the width of the peak is approximately 0.8^o.
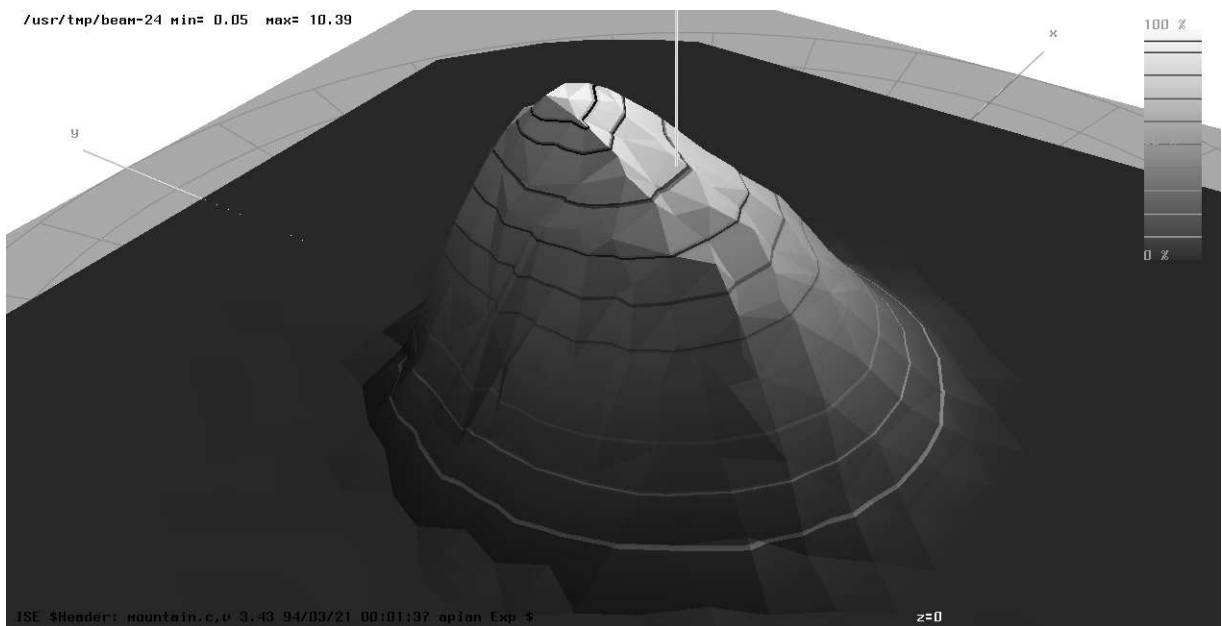

Fig. 11. Profile of the xenon lamp beam

7. DISCUSSION

The basic design of the apparatus has proven to be reliable so far, with some minor corrections incorporated. The measured data covers material types used for new window materials and forms the basis on which modelling and simulation calculations are based. Planned extensions include sample holders for measuring thermotropic glazings, new ammeters and spectral extensions.

8. ACKNOWLEDGEMENTS
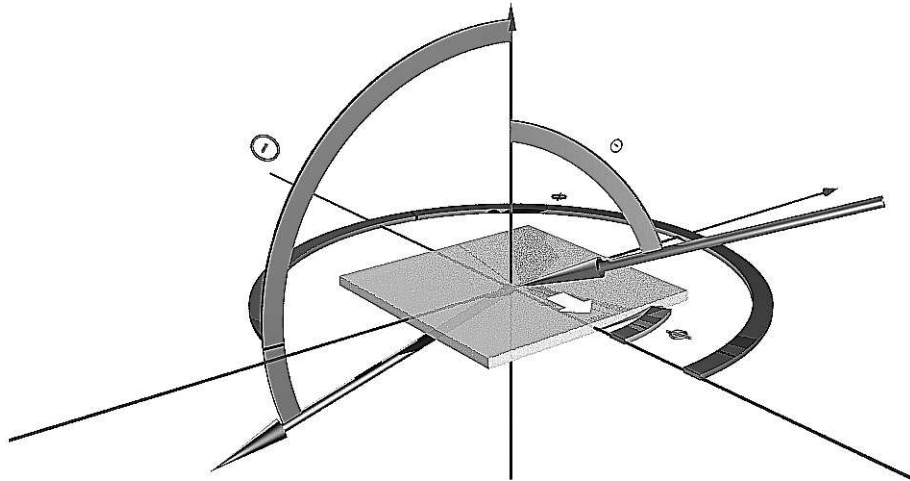
9. APPENDICES

Fig. 12. Coordinate system used

10. REFERENCES

1   P. Apian-Bennewitz, "Bau einer Apparatur zur Messung winkelabhängiger Licht-Streuung in anisotropen Medien", diploma-thesis, Univ. Freiburg, 1990

2   J. Dengler, P. Apian-Bennewitz, W. Platzer, V. Wittwer, "Advanced Transparent Insulation Materials", Sixth International Meeting on Transparent Insulation Technology Ti6, 3-5 June 1993, Birmingham

3   A. Häberle, A. Gerber, T. Schmidt, P. Apian-Bennewitz, V. Wittwer, "The Amount Of Solar Radiation Absorbed By Trough Collectors With Non-imaging Optics", Fhg-ISE, to be published in this SPIE proceedings

4   K.M. Papamichael, S.E. Selkowitz, "Simulating the Luminous and Thermal Performance of Fenestration Systems", Lawrence Berkeley Lab 1987

5   K.M. Papamichael, F. Winkelmann, "Solar-Optical Properties of Multilayer fenestration Systems", Lawrence Berkeley Lab, Applied Science Div., 1986

6   K.M. Papamichael, J. Klems, S. Selkowitz, "Determination and Application of Bidirectional Solar-Optical Properties of Fenestration Systems", Proc. of 13th National Passive Solar Conference, Cambridge MA, June 19-24 1988

7   T. Schmidt, "Optische Charakterisierung transparenter Materialien im Hinblick auf eine Auswertemethode experimenteller Streudaten", diploma thesis, Univ. Freiburg, 1993

8   J. Weese, "A reliable and fast method for the solution of Fredholm integral equations of the first kind based on Tikhonov regularization", Comp. Phys. Comm., Vol 69, p 99-111, 1992

9   H.R. Wilson, W. Eck, "Light transmission control with thermotropic layers", 1993 Solar World Congress, Proc. of the Biennial Congress of the International Solar Energy Society (ISES), Budapest, Ungarn, 23.-27.8.1993